JOURNAL OF MATERIALS SCIENCE **28** (1993) 632–638

Chemical and structural properties of the system Fe_2O_3–Cr_2O_3

S. MUSIĆ, S. POPOVIĆ*, M. RISTIĆ
*Rudjer Bošković Institute, P. O. Box 1016, *and also Physics Department, Faculty of Science, PO Box 162, 41001 Zagreb, Croatia*

Chemical and structural properties of the mixed metal oxides $(1-x)Fe_2O_3+xCr_2O_3$ were studied by different techniques. X-ray powder diffraction showed the existence of solid solutions, $(Fe_{1-x}Cr_x)_2O_3$, over the whole concentration region, $0 \leqslant x \leqslant 1$. The gradual replacement of Fe^{3+} with Cr^{3+} ions in samples prepared at 900 °C caused changes in unit-cell parameters; most of these changes took place in the region from $x \approx 0.3$–0.9. The samples having the fraction of Cr_2O_3 in the region from ~0.7–0.8, contained two closely related phases, with slightly different compositions. After an additional heat treatment at 1100 °C, these samples contained only one phase. ^{57}Fe Mössbauer spectroscopy showed a gradual decrease of hyperfine magnetic field with increasing Cr_2O_3 content. The sample having the fraction of Cr_2O_3 of 0.7, and prepared at 900 °C, exhibited two separated sextets at room temperature, in comparison with other compositions showing one sextet. It was shown that Fourier transform–infrared (FT–IR) spectroscopy is a powerful method for the investigation of structural changes in these solid solutions. The increase in the Cr_2O_3 content resulted in shifts of the corresponding infrared bands. In addition, a gradual transition of the spectrum typical for α-Fe_2O_3 to the spectrum typical for Cr_2O_3 was shown. The transition effects observed in the FT–IR spectra were correlated with the X-ray powder diffraction and ^{57}Fe Mössbauer spectroscopic results.

1. Introduction

Investigation of chemical, physical and structural properties of mixed metal oxides is very important, because this group of compounds has found very important applications in new technologies, or simply, they could be perspective materials in the future. For instance, superior technical ceramics, materials for magnetic recording, many electronic components, sensors and catalysts, as well as the high-temperature superconductors, are based on the structure of mixed metal oxides. Specific physical behaviour of many mixed metal oxides can be considered as a function of their specific chemical and structural properties. For this reason, many researchers have paid attention to different methods of the synthesis of mixed metal oxides and their characterization.

Musić *et al.* [1] investigated the system Fe_2O_3–Ga_2O_3 using X-ray diffraction and ^{57}Fe Mössbauer spectroscopy. The samples were heated to 600 °C. The presence of only one phase, α-$(Fe_{1-x}Ga_x)_2O_3$, was detected for the compositions with $x = 0$ to ~0.95. A gradual decrease of the unit-cell parameters of α-$(Fe_{1-x}Ga_x)_2O_3$ and the reduction of the hyperfine magnetic field, HMF, with an increase in the amount of gallium were observed. The hyperfine magnetic structure, which was observed for α-$(Fe_{1-x}Ga_x)_2O_3$ at room temperature, collapsed for the composition with $x \approx 0.50$. The changes in the ^{57}Fe Mössbauer spectra of the α-$(Fe_{1-x}Ga_x)_2O_3$ phase were discussed in terms of the electronic relaxation and the superparamagnetic effects.

The system Fe_2O_3–In_2O_3 was also investigated [2] using X-ray diffraction, ^{57}Fe Mössbauer spectroscopy and infrared spectroscopy. The chemistry of Ga^{3+} and In^{3+} ions is very similar. However, the ionic radius of In^{3+} (0.092 nm) is significantly greater than those of Fe^{3+} (0.067 nm) and Ga^{3+} (0.062 nm). For this reason, different effects of In^{3+} ions on the α-Fe_2O_3 structure, in relation to Ga^{3+} ions, were expected. For the samples heated at 600 °C, a phase, α-$(Fe_{1-x}In_x)_2O_3$, isostructural with α-Fe_2O_3, existed for $0 \leqslant x \lesssim 0.8$, and a phase C-$(Fe_{1-x}In_x)_2O_3$, isostructural with cubic In_2O_3, existed for $0.3 \lesssim x \leqslant 1$. In the two-phase region these two phases were poorly crystallized. For the samples heated at 900 °C the two-phase region was wider and existed for $0.1 \lesssim x \leqslant 0.8$ with two phases well crystallized. ^{57}Fe Mössbauer spectroscopy of samples prepared at 600 °C indicated a general tendency of the broadening of spectral lines and a decrease of the HMF values with increasing molar content of In_2O_3. The samples prepared at 900 °C, in the two-phase region, were characterized by a constant HMF value, 510 kOe, at room temperature. Differences in the chemical and structural behaviour between the systems Fe_2O_3–Ga_2O_3 and Fe_2O_3–In_2O_3 are dominantly influenced by the differences in the ionic radii of Ga^{3+} and In^{3+}.

Investigation of the system Fe_2O_3–SnO_2 showed [3] that there is no affinity between Fe^{3+} and Sn^{4+} ions to form solid solutions, in spite of the fact that the ionic radii of Fe^{3+} and Sn^{4+} ions do not differ. It was concluded that the similarity of ionic radii of metal cations is a dominant factor in the formation of solid solutions, if different metal cations form the same type of crystal structure. On the other hand, the ionic radii of the metal cations are not a dominant factor in the formation of solid solutions, if two metal cations form different types of oxide crystal structure. An example of this, is the system Fe_2O_3–SnO_2, where Sn^{4+} ions do not favour the structure α-Fe_2O_3, and Fe^{3+} ions do not favour the structure of SnO_2.

In the systems Fe_2O_3–Ln_2O_3, Ln = Eu or Gd, four distinct crystalline phases were detected, namely α-Fe_2O_3, $Ln_3Fe_5O_{12}$, $LnFeO_3$ and Ln_2O_3. No solid solutions were observed. Under certain experimental conditions a fraction of an amorphous phase was also present [4, 5]. New accurate crystal powder data for $Gd_3Fe_5O_{12}$ were given [5]. Mössbauer spectroscopy showed significant differences between the samples prepared in the system Fe_2O_3–Eu_2O_3 or Fe_2O_3–Gd_2O_3, due to the presence of different oxide phases in these samples.

The aim of present work was to obtain information about chemical and structural properties of the system $(1 - x)Fe_2O_3 + xCr_2O_3$, as a function of x. Fe(III) and Cr(III) oxides form corundum (α-Al_2O_3) type of crystal structure. For this reason, the formation of solid solutions in the system Fe_2O_3–Cr_2O_3 over the whole concentration range is expected. X-ray diffraction, Mössbauer spectroscopy and Fourier transform–infrared (FT–IR) spectroscopy were used as experimental techniques.

2. Experimental procedure

Analar reagent grade chemicals and doubly distilled water were used. Samples were prepared using the following procedure. $Fe(OH)_3/Cr(OH)_3$ coprecipitates were carefully washed using a Sorvall-RC2-B ultraspeed centrifuge, up to 20000 r.p.m. After drying, the hydroxide coprecipitates were heated for 1 h each at 200, 300, 500 and 600 °C, and for 4 h at 900 °C ("step-by-step" heating). The thermal treatment of samples at 1100 °C for 2 h was performed using the high-temperature furnace LKO II with Kanthal heaters. The samples in the form of powder were sintered using a 10 t press, before heating at 1100 °C. The chemical composition of samples S-1 to S-14 prepared in the system $(1 - x)Fe_2O_3 + xCr_2O_3$, $0 \leqslant x \leqslant 1$, is given in Table I.

TABLE I Chemical composition of the samples prepared in the system $(1 - x)Fe_2O_3 + xCr_2O_3$

Sample	Molar fraction	
	Fe_2O_3	Cr_2O_3
S-1	0.99	0.01
S-2	0.97	0.03
S-3	0.95	0.05
S-4	0.90	0.10
S-5	0.85	0.15
S-6	0.80	0.20
S-7	0.75	0.25
S-8	0.70	0.30
S-9	0.50	0.50
S-10	0.30	0.70
S-11	0.20	0.80
S-12	0.10	0.90
S-13	0.05	0.95
S-14		1

X-ray diffraction (XRD) powder patterns were taken at room temperature using a counter diffractometer with monochromatized CuK_α radiation (Philips diffractometer, proportional counter and graphite monochromator).

^{57}Fe Mössbauer spectra were recorded using a commercial Mössbauer spectrometer WISSEL. A ^{57}Co–Rh source (Amersham) was used. The standard absorbers, α-Fe, α-Fe_2O_3 and ^{57}Fe/Rh (Amersham) were also used.

All FT–IR spectra were recorded using a Fourier transform IR spectrometer 1720-x made by Perkin-Elmer. The specimens were pressed in KBr discs. In this paper the FT–IR spectra are presented as relative transmission versus the wave number (cm^{-1}).

3. Results and discussion

The ionic radii of iron and chromium are very similar: 0.067 nm for Fe^{3+} and 0.064 nm for Cr^{3+}. The compounds α-Fe_2O_3 and Cr_2O_3 (mineral names haematite and eskolaite, respectively) belong to the same space group, i.e. they are isostructural having rhombohedral symmetry $R\,\bar{3}\,c$ (no. 167). The unit-cell parameters are also very similar, and their values are given in Table II. The difference in the a parameters is 1.59% and the difference in the c parameters is 1.22%. The unit-cell parameters of α-Fe_2O_3 and Cr_2O_3, measured in this work, were practically equal to the literature data given in Table II. For this reason, the literature data were used for calibration of the angular scale of the diffractometer. X-ray diffraction analysis showed that over the whole concentration range, solid solutions of the type $(Fe_{1-x}Cr_x)_2O_3$ were formed. These solid solutions were isostructural with α-Fe_2O_3 and Cr_2O_3. All samples heated at 900 °C were one-phase systems, except samples S-10 and S-11, which

TABLE II Crystallographic data for α-Fe_2O_3 and Cr_2O_3 [6]

JCPDS PDF card no.	Compound	Space group	Unit-cell parameters at 25 °C (nm)
13-534	α-Fe_2O_3	$R\bar{3}c$	Hexagonal axes $a = 0.5034$ $c = 1.3752$
6-504	Cr_2O_3	$R\bar{3}c$	Hexagonal axes $a = 0.4954$ $c = 1.3584$

consisted of two closely related phases, having slightly different composition. The separation of the analogous diffraction lines of the two phases was visible only at higher Bragg angles. After an additional heat treatment at 1100 °C samples S-10 and S-11 contained only one phase.

The replacement of Fe^{3+} with Cr^{3+} ions was manifested in small shifts of diffraction lines toward higher Bragg angles, i.e. a decrease of the unit-cell parameters took place. These changes were very small in the iron-rich region, up to sample S-8 (the molar fraction of Fe_2O_3 varies from 1 to ~ 0.70), and in the chromium-rich region, from sample S-12 to sample S-14 (the molar fraction of Fe_2O_3 varies from ~ 0.10–0). The main changes in unit-cell parameters took place in the region from sample S-8 to sample S-12 (the molar fraction of Fe_2O_3 varies from ~ 0.70 to ~ 0.10). Diffraction lines of samples S-9 to S-12 were slightly broadened, but after additional heating at 1100 °C these samples exhibited sharp diffraction lines, well-resolved into the spectral doublet components $K\alpha_1\alpha_2$.

Sample S-14 showed the same diffraction pattern as the sample of Cr_2O_3 (99.999%) from Ventron.

^{57}Fe Mössbauer spectra of samples S-1 to S-10 are shown in Figs 1 and 2. Hyperfine magnetic fields (average values), measured for samples S-1 to S-10, are given in Table III. ^{57}Fe Mössbauer spectra of samples S-1 and S-2 were very similar to the spectrum of pure α-Fe_2O_3. Hyperfine magnetic fields measured for samples S-1 and S-2 (up to 3 mol % Cr_2O_3) were in accordance with the value (517 kOe) measured for the well-crystallized α-Fe_2O_3. With further increase of the molar content of Cr_2O_3 there was gradual decrease in the value of hyperfine magnetic field. A gradual broadening of spectral lines was also characteristic of these spectra. ^{57}Fe Mössbauer spectrum of sample S-10 recorded at room temperature, indicated a clear separation of one sextet into two sextets. The results of ^{57}Fe Mössbauer spectroscopy indicated a gradual increase of non-equivalent ^{57}Fe sites inside one oxide particle with increasing content of Cr^{3+} ions in the α-Fe_2O_3 structure. The contributions of these ^{57}Fe nucleides to the Mössbauer effect are different. Two sextets, recorded for sample S-10, indicated the presence of two different oxide phases inside one and the same particles, having the average composition $(Fe_{0.3}Cr_{0.7})_2O_3$.

Srivastava and Sharma [7] prepared samples in the system Cr_2O_3–Fe_2O_3 containing 1.77, 3.85, 5.66 or 7.41 wt % Fe_2O_3. Mössbauer measurements showed a distinct deviation of spectral lines from Lorentzian shape, as well as an increased intensity of the central part of the spectrum. The intensity of the central part of the Mössbauer spectrum of the solid solutions Cr_2O_3–Fe_2O_3 decreased with increasing annealing time or temperature, or when the samples were quenched to room temperature. It was suggested that an incomplete annealing of Cr_2O_3 matrix containing Fe^{3+} ions produced a non-uniform distribution of Fe^{3+} ions in the Cr_2O_3 matrix. Such an inhomogeneous diffusion of Fe^{3+} ions might cause the formation of clusters which exhibited the superparamagnetism. In the paper by Srivastava and Muralidhara Rao [8] another possible mechanism of annealing of the solid solution Cr_2O_3–3.85 wt % Fe_2O_3 was suggested. The authors assumed that an annealing temperature of 1250 °C was sufficient to cause a uniform distribution of Fe^{3+} ions in the Cr_2O_3 matrix. However, when the solid solution was slowly cooled to room temperature after annealing, Fe^{3+} ions clustered back to the original lattice sites.

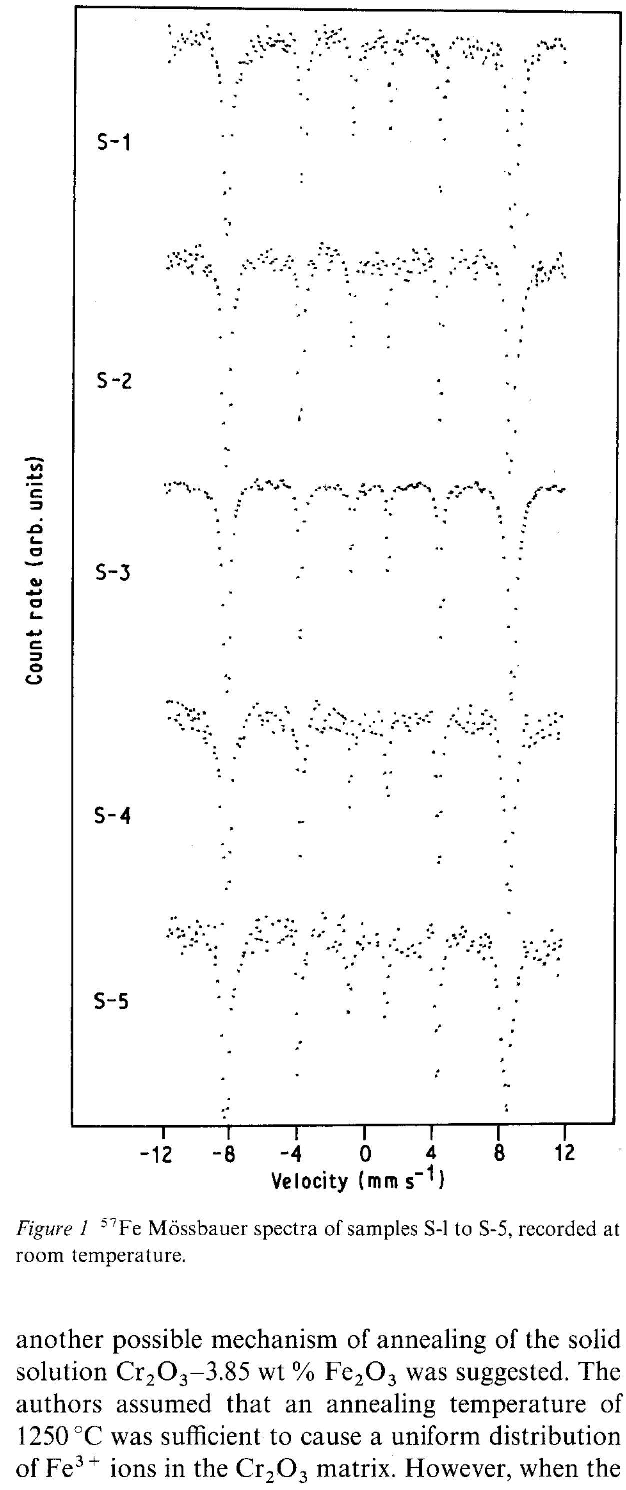

Figure 1 ^{57}Fe Mössbauer spectra of samples S-1 to S-5, recorded at room temperature.

Doppler *et al.* [9]. investigated different types of high-temperature water–gas shift catalysts and their precursors using different physical methods and Mössbauer spectroscopy. ^{57}Fe Mössbauer spectrum of the solid solution $Fe_yCr_{2-y}O_3$ recorded at room temperature, consisted of two sextets and the central quadrupole doublet of small intensity. The outer sextet was ascribed to the approximate composition $Fe_{1.8}Cr_{0.2}O_3$, and the inner sextet to the non-uniform composition $Fe_yCr_{2-y}O_3$, $1 < y < 1.8$. At room temperature, for the outer sextet $H_{5/2} = 495$ kOe and for the inner sextet $H_{5/2} = 454$ kOe were measured. Used catalysts showed Mössbauer spectra typical for magnetite of varying stoichimetry, $Fe_{3-x}O_4$. Mössbauer

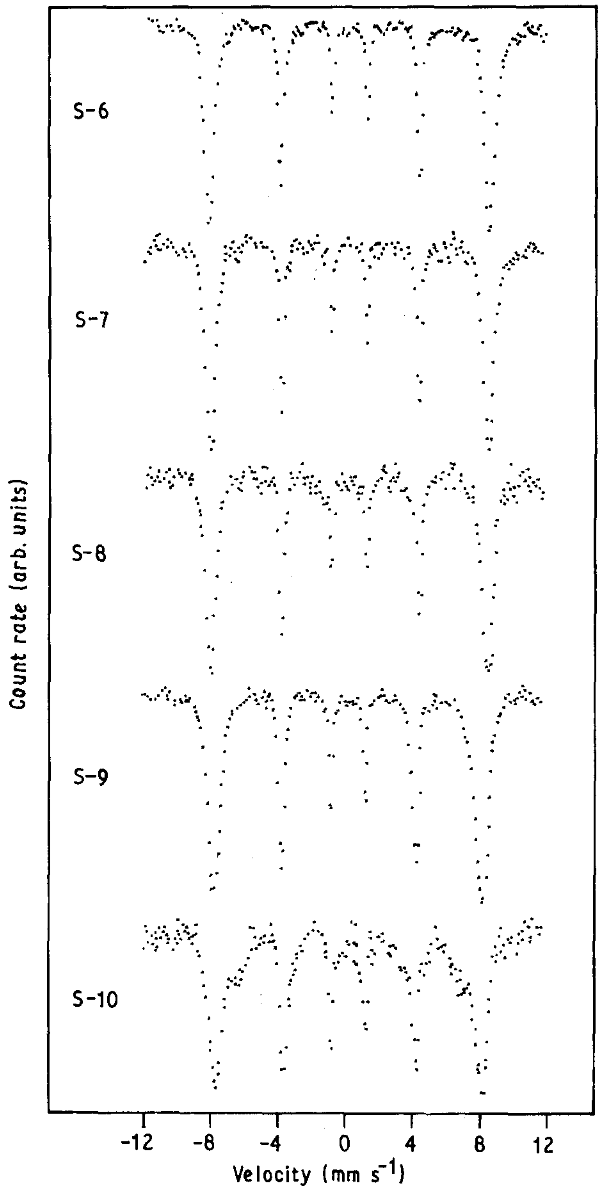

Figure 2 ^{57}Fe Mössbauer spectra of samples S-6 to S-10, recorded at room temperature.

TABLE III Hyperfine magnetic fields (average values) for samples S-1 to S-10, measured at room temperature (± 2kOe)

Sample	M_1(kOe)	M_2(kOe)
S-1	517	
S-2	517	
S-3	516	
S-4	511	
S-5	510	
S-6	505	
S-7	503	
S-8	500	
S-9	486	
S-10	480	421

spectroscopy was also used in the investigation of different forms of magnetite catalysts for water–gas shift reaction, in which carbon monoxide reacts with steam to yield carbon dioxide and hydrogen [10].

In our previous paper [2] we showed that infrared spectroscopy could be used to follow chemical and structural changes in the mixed metal oxides Fe_2O_3–In_2O_3. In the present work we used FT–IR spectroscopy to follow chemical and structural changes in the mixed metal oxides Fe_2O_3–Cr_2O_3. On the basis of literature data, the main characteristics of the vibrational spectra of α-Fe_2O_3 and α-Cr_2O_3 will be reviewed. This is important for a better understanding of the changes in the FT–IR spectra recorded for the samples prepared in the system (1–x) Fe_2O_3 + $x Cr_2O_3$.

The infrared spectrum of lath-shaped α-Fe_2O_3 particles showed infrared absorption bands at 525, 440, 300 and 229 cm^{-1}, which were assigned to E_u vibration modes [11]. Infrared bands at 650 and 400 cm^{-1} were assigned to A_{2u} vibration modes. α-Fe_2O_3 produced by heating α-FeOOH at 950 °C was characterized by a complex morphology, due to interparticle sintering that occurred at higher temperatures (700–1000 °C). The complex morphology of these α-Fe_2O_3 particles was confirmed by electron microscopy. The infrared spectrum of these α-Fe_2O_3 particles showed three strong infrared bands at 540, 470 and 355 cm^{-1}, a weak infrared band at 380 cm^{-1} and a shoulder at 630 cm^{-1}.

Iglesias *et al.* [12] investigated the influence of aggregation of α-Fe_2O_3 particles on the corresponding infrared spectrum. When homogeneous aggregation was assumed, the frequency of the infrared bands decreased, together with a certain increase in their widths. The broadening of infrared bands was even greater when heterogeneous clustering was considered. Other infrared spectroscopic investigations concerning α-Fe_2O_3 were reviewed in our previous publication [2].

Serna *et al.* [11] recorded infrared spectra for α-Cr_2O_3 particles of different morphology. For lath-like morphology, dominant infrared bands at 617, 556, 443 and 305 cm^{-1} were assigned to E_u vibration modes, and those at 415 and ~720 cm^{-1} to A_{2u} vibration modes. The appearance of a shoulder at 650–700 cm^{-1} is due to the presence of α-Cr_2O_3 particles in the form of cylinders and spheres. In a case of a large proportion of spherical α-Cr_2O_3 particles, a distinct infrared band at 600 cm^{-1} was observed.

Infrared reflectivity measurements on a single crystal of Cr_2O_3 were performed at room temperature [13]. The modes vibrating perpendicular to the c-axis had positions at 417, 444, 532 and 613 cm^{-1}, while the modes vibrating parallel to the c-axis had positions at 538 and 613 cm^{-1}.

Ottesen [14] used FT–IR reflectance spectroscopy in the study of oxide films formed on the surface of binary iron–chromium alloys. The author concluded that some features observed in the reflectance infrared spectra could be misleadingly interpreted, if compared with classical infrared spectra. These differences are caused by several factors, such as the larger and rapidly varying indexes of reflection for metal oxides, the rough nature of the oxide films, the presence of complex oxide phases, as well as by experimental factors such as the angle of incidence, angle of divergence and beam polarization. The following infrared bands were found in FT–IR reflectance spectra of a Cr_2O_3 film: 400, 600, 735 and 530 cm^{-1}. It was suggested that the infrared at 530 cm^{-1} is suitable for thickness determination of a Cr_2O_3 film.

Lenglet *et al.* [15] investigated oxidation products of stainless steel 18Cr–10Ni–2Mn, formed in air between 900 and 1000 °C. Different oxidation products were detected, such as Cr_2O_3, $MnCr_2O_4$, Fe_2O_3, as well as Fe_3O_4 in the early stage of the oxidation of the steel surface. On the basis of FT–IR reflectance spectra, the following infrared bands were used in phase identification: 745–730 cm^{-1} for Cr_2O_3, 690, 590 and 470–460 cm^{-1} for chromite, and 510 and 430–420 cm^{-1} for α-Fe_2O_3.

Infrared spectroscopy was also applied in the investigation of magnetite containing Cr^{3+} ions and of their oxidation products [16–20].

The results of FT–IR spectroscopic measurements, obtained in the present work, are summarized in Figs 3–7. FT–IR spectra of samples S-1 and S-2 were similar to the infrared spectrum of haematite. Sample S-2 was characterized with two dominant infrared bands at 555 and 480 cm^{-1}, with a visible shoulder at 630 cm^{-1}. In the infrared spectrum of sample S-2 there was also an infrared band of weak intensity at 390 cm^{-1}. The main characteristics of the FT–IR spectrum of sample S-3 were two dominant infrared bands at 548 and 478 cm^{-1} with well-pronounced shoulders at 632 and 464 cm^{-1}. The shape of the FT–IR spectra did not change up to sample S-8; however, there were gradual shifts of infrared bands with increasing molar contents of Cr_2O_3. For instance, dominant infrared bands at 555 and 480 cm^{-1} (sample S-2) shifted to 573 and 499 cm^{-1} (sample S-8). In the FT–IR spectrum of sample S-9, the following changes appeared in relation to the previous spectra.

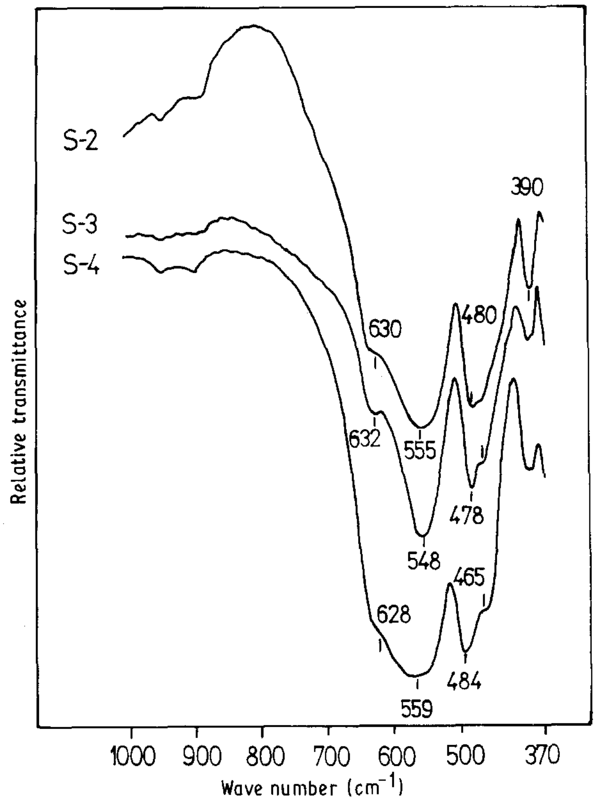

Figure 3 FT–IR spectra of samples S-2 to S-4, recorded at room temperature.

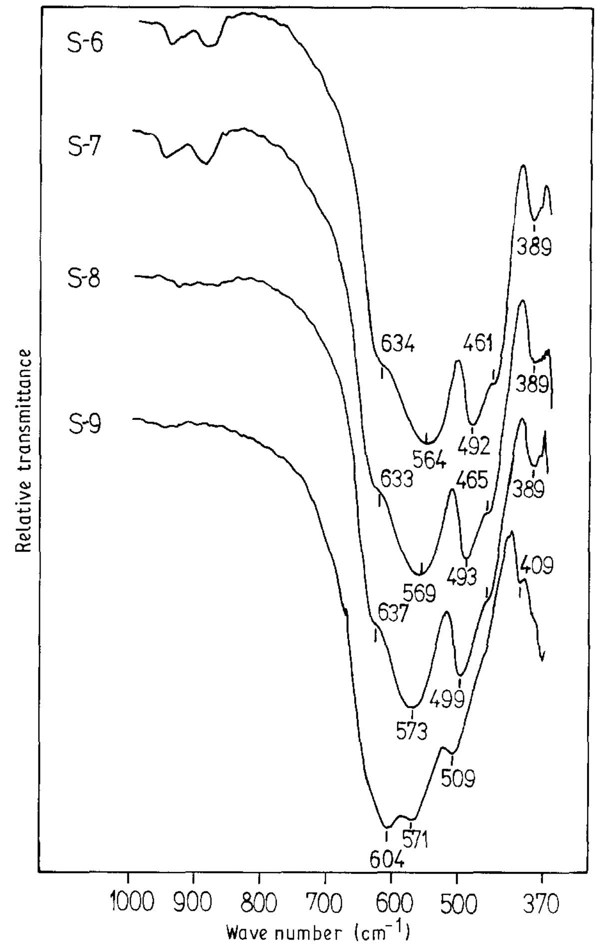

Figure 4 FT–IR spectra of samples S-6 to S-9, recorded at room temperature.

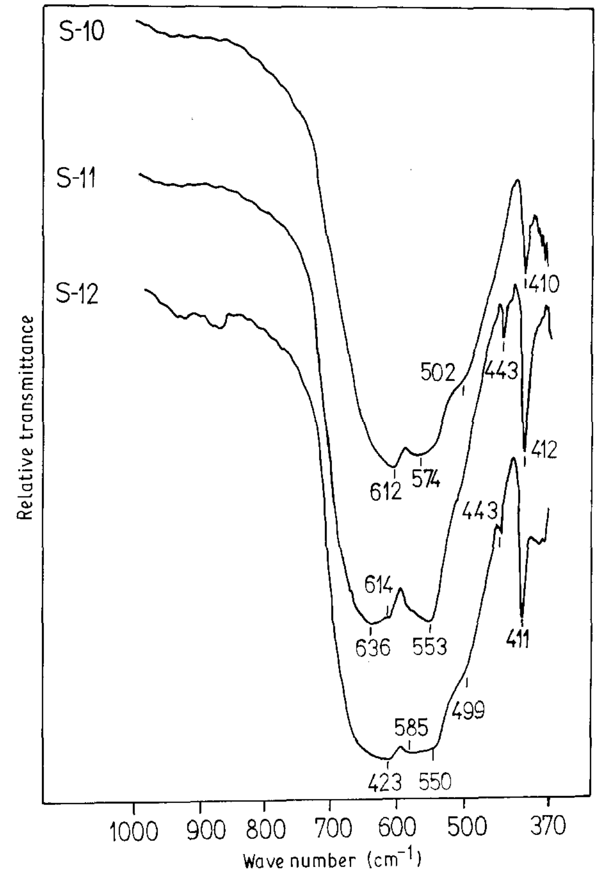

Figure 5 FT–IR spectra of samples S-10 to S-12, recorded at room temperature.

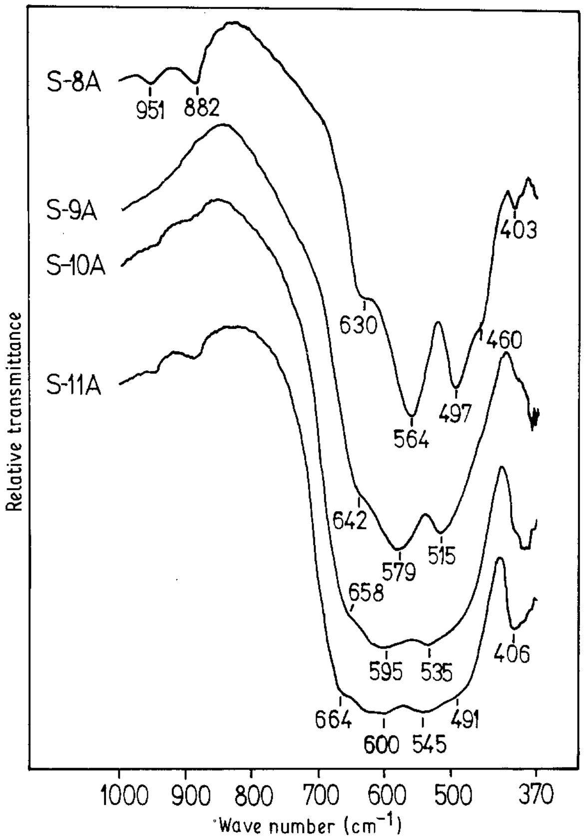

Figure 6 FT–IR spectra of samples S-8A to S-11A, recorded at room temperature.

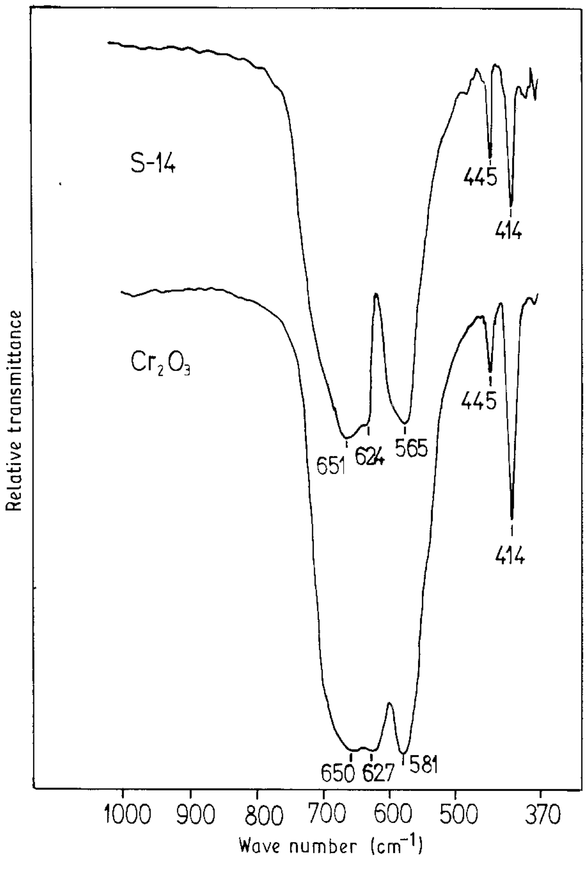

Figure 7 FT–IR spectra of sample S-14 and Cr_2O_3 (99.999%, Ventron), recorded at room temperature.

A new infrared band at 409 cm^{-1} appeared, which is characteristic of α-Cr_2O_3. In the same spectrum, a strong infrared band with transmission minima at 604 and 571 cm^{-1} appeared, as well as the infrared band at 509 cm^{-1} which had position at 499 cm^{-1} in sample S-8. The FT–IR spectrum of sample S-10 was characterized with a very strong and broad infrared band with transmission minima at 612 and 574 cm^{-1} and a shoulder at 502 cm^{-1}. The intensity of the infrared band at 410 cm^{-1} increased significantly in relation to the same infrared band in the spectrum of sample S-9.

Evidently, FT–IR spectra of sample S-9 and particularly of sample S-10 indicate the transition between the structures (solid solutions) of α-Fe_2O_3 and Cr_2O_3, but with spectral characteristics of both structures. In the FT–IR spectra of samples S-11 and S-12, the infrared band at 443 cm^{-1}, characteristic of the α-Cr_2O_3 structure, was well pronounced. The transition effects observed in these FT–IR spectra can be correlated with X-ray diffraction and Mössbauer spectroscopic results. A typical example is sample S-10.

Fig. 6 shows FT–IR spectra of samples S-8A to S-11A. These samples were prepared by sintering samples S-8 to S-11 in the powdered state and their additional heating at 1100 °C for 2 h. The FT–IR spectrum of sample S-8A was similar to the spectrum of sample S-8. In the FT–IR spectra of samples S-9A to S-11A the corresponding infrared bands were gradually broadened. The sintering and additional heating at 1100 °C of samples S-9, S-10 and S-11 caused a disappearance of sharp bands at 410 and 443 cm^{-1}, which are characteristic of the α-Cr_2O_3-type structure. These results are in full accordance with the X-ray diffraction analysis described previously.

The FT–IR spectrum of sample S-14 corresponded to Cr_2O_3. For comparison the FT–IR spectrum of commercial Cr_2O_3 (99.999%) by Ventron was also recorded and was found to be very similar to that of sample S-14 (Fig 7).

References

1. S. MUSIĆ, S. POPOVIĆ and M. RISTIĆ, *J. Mater. Sci.* **24** (1989) 2722.
2. M. RISTIĆ, S. POPOVIĆ, M. TONKOVIĆ and S. MUSIĆ *ibid.* **26** (1991) 4225.
3. S. MUSIĆ, S. POPOVIĆ, M. METIKOŠ-HUKOVIĆ and V. GVOZDIĆ, *J. Mater. Sci. Lett.* **10** (1991) 197.
4. M. RISTIĆ, S. POPOVIĆ and S. MUSIĆ, *ibid.* **9** (1900) 872.
5. S. MUSIĆ, V. ILAKOVAC, M. RISTIĆ and S. POPOVIĆ, *J. Mater. Sci.* **27** (1992) 1011.
6. International Centre for Diffraction Data, Joint Committee on Powder Diffraction Standards, Powder Diffraction File, 1601 Park Lane, Swarthmore, PA, 19081, USA.
7. J. K. SRIVASTAVA and R. P. SHARMA, *J. Physique* **35** (1974) C6-663.
8. J. K. SRIVASTAVA and S. MURALIDHARA RAO, *Phys. Status Solidi* (*b*) **90** (1978) K175.
9. G. DOPPLER, A. X. TRAUTWEIN, H. M. ZIETHEN, E. AMBACH, R. LEHNERT and M. J. SPRAGUE, *Appl. Catal.* **40** (1989) 119.
10. D. G. RETHWISCH, J. PHILLIPS, Y. CHEN, T. F. HAYDEN and J. A. DUMESIC, *J. Catal.* **91** (1985) 167.
11. C. J. SERNA, J. L. RENDON and J. E. IGLESIAS, *Spectrochim. Acta* **38A** (1982) 797.
12. J. E. IGLESIAS, M. OCANA and C. J. SERNA, *Appl. Spectros.* **44** (1990) 418.
13. D. R. RENNEKE and D. W. LYNCH, *Phys. Rev.* **138** (1965) A530.

14. D. K. OTTESEN, *J. Electrochem. Soc.* **132** (1985) 2250.
15. M. LENGLET, R. GUILLAMET, J. LOPITAUX and B. HANNOYER, *Mater. Res. Bull.* **25** (1990) 575.
16. B. GILLOT, F. BOUTON, F. CHASSAGNEUX and A. ROUSSET, *J. Solid State Chem.* **33** (1980) 245.
17. B. GILLOT, F. BOUTON, J. F. FERRIOT, F. CHASSAGNEUX and A. ROUSSET, *ibid.* **21** (1977) 375.
18. B. GILLOT, F. JEMMALI and A. ROUSSET, *ibid.* **50** (1983) 138.
19. F. CHASSAGNEUX, A. ROUSSET and J. P. REDOULES, *ibid.* **56** (1985) 74.
20. B. GILLOT, F. JEMMALI, M. LAARJ, F. CHASSAGNEUX and A. ROUSSET, *J. Mater. Sci.* **23** (1988) 872.

Received 19 July 1991
and accepted 11 March 1992